Transport and relaxation of hot conduction electrons in an organic dielectric

E. Cartier and P. Pfluger
Brown Boveri Research Center, CH-5405 Baden, Switzerland
(Received 13 June 1986)

Effective mean free paths of hot electrons in the energy range 0.5 eV $\leq E_{kin} \leq$ 20 eV are determined experimentally for the paraffin n-$C_{36}H_{74}$ with the internal photoemission for transport analysis method. The hot-electron transport parameters are discussed in terms of fundamental scattering mechanisms in organic dielectrics. The influence of hot-electron-induced trap formation on the transport properties is investigated. The consequences for dielectric breakdown are pointed out.

I. INTRODUCTION

The importance of the transport properties of hot electrons for dielectric breakdown in terms of the avalanche breakdown model was discussed in detail in previous papers.[1,2] It has been shown that relevant quantities such as the mean kinetic energy, the electron multiplication rate, and the breakdown field of dielectrics can be calculated if the energy- and momentum-loss rates, $\gamma_u(E_{kin})$ and $\gamma_p(E_{kin})$, of electrons with kinetic energies ranging from $\sim kT$ up to the intergap excitation threshold are known. Sparks *et al.*[1] calculated energy- and momentum-loss rates in alkali halides and consistently explained laser breakdown in terms of the avalanche model. A comparable calculation appears very involved for organic dielectrics since many individual scattering channels would have to be taken into account. The scattering due to the emission of high-frequency optical phonons can, in principle, be described theorectically given some knowledge on the relevant energy-loss processes for electrons with energies in the eV range in hydrocarbons.[3] On the other hand, an analytical description of $\gamma_p(E)$ seems to be out of reach at present. Therefore, the method of internal photoemission for transport analysis (IPTA) has been developed in our laboratory in order to determine energy- and momentum-loss rates in organic dielectrics experimentally.[4] The IPTA method was successfully applied to the linear alkane hexatriacontane, n-$C_{36}H_{74}$, which was chosen for the experiments due to its model character for polyethylene.[5] The IPTA method is based on the injection of hot electrons into the conduction band of insulators at a metal-dielectric interface and the measurement of energy distributions of electrons transmitted through insulating films of varying thickness. The changes of the energy distributions contain information about the scattering events inside the dielectric. The energy-level diagram of the internal photoemission experiments for transport analysis is shown in Fig. 1.

In order to quantitatively determine transport parameters from the measured energy distributions, the Boltzmann transport equation, with appropriate boundary and initial conditions for the plane-layer configuration used in the IPTA experiments has to be solved. However, it is not necessary to solve the problem in its full generality. For the topmost energy interval ($E_{max}-\Delta E$, E_{max}) of the energy distribution (ΔE is a characteristic energy loss in the dielectric), electrons are scattered out of the interval by inelastic collisions but none are scattered into this interval from higher energies. This fact simplifies the analysis and yields the following asymptotic expressions for the intensity of electrons transmitted at the topmost energy interval through a dielectric film of thickness d (Ref. 4):

$$I(d)/I(0) \sim \begin{cases} 1-({}^1/l_u + {}^1/l_p)d, & \text{as } d \to 0 \quad (1a) \\ \exp(-d/\lambda_{eff}) & \text{as } d \to \infty\ , \quad (1b) \end{cases}$$

$$\lambda_{eff} = \tfrac{1}{2}(l_u l_p)^{1/2}\ . \quad (2)$$

The inelastic and elastic scattering lengths, l_u and l_p, are

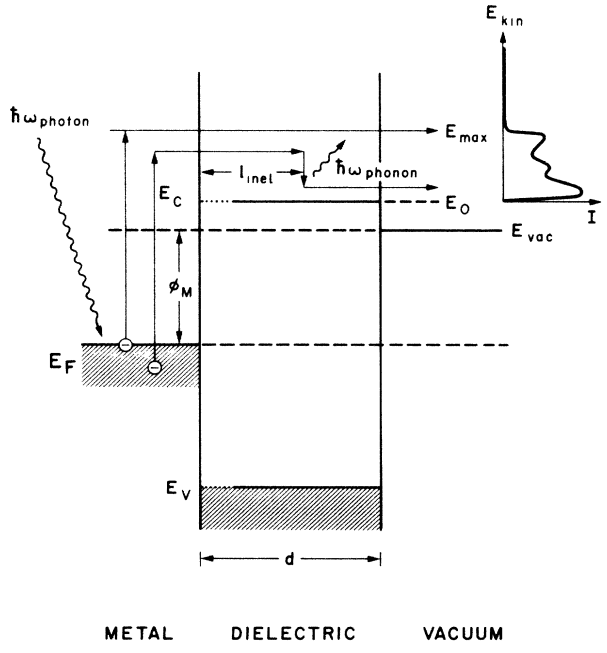

FIG. 1. Energy-level diagram of the IPTA (internal photoemission for transport analysis) experiment. In our case, polycrystalline Pt was used as electron emitter, and the long chain paraffine n-$C_{36}H_{74}$ as dielectric.

 ©1986 The American Physical Society

related to the loss rates by the expression $l_{u,p} = \gamma_{u,p}^{-1}(2E/m^*)^{1/2}$. The energy dependence of the transport properties is scanned by varying the energy position of the topmost energy interval. The effective scattering length, λ_{eff}, is determined by the exponential thickness dependence of the intensity at $E_{\max}$ for large film thickness as given by formula (1b). As can be seen from the formalism derived in Refs. 1 and 2, the product $l_u l_p$ (or $\gamma_u \gamma_p$) is the only non trivial quantity required for the calculation of breakdown properties. Therefore, the separation of l_u and l_p is not necessary within the framework of avalanche breakdown.

The experiments published previously[4] were restricted to electron kinetic energies $E_{\text{kin}} \leqq 2.4$ eV. We now present the extension of IPTA experiments up to kinetic energies of about 20 eV, covering the whole energy range required for the calculation of breakdown properties in terms of avalanche breakdown.

After giving some experimental details in Sec. II, we also discuss the influence of hot carrier induced radiation damage on the experimental results (Sec. III). Radiation damage during experimental transport studies of electrons above 3.5 eV kinetic energy appears to be inevitable and has to be taken into account when interpreting experimental results. In Sec. IV experimental results of hot-electron transport are presented. Finally, these results are discussed with respect to various scattering processes in dielectrics as well as with respect to experimental and theoretical work on inorganic insulators.

II. EXPERIMENTAL

The experiments were performed on a KRATOS ES300 photoelectron spectrometer with a special analysis mode for low-energy electrons. Polycrystalline Pt was evaporated *in situ* as injector. Its work function was monitored until perfect matching with the dielectric was obtained by contamination in the submonolayer range. This procedure guarantees flat band conditions at the metal/solidus dielectric interface. Then dielectric films (high-purity linear alkane n-$C_{36}H_{74}$) were evaporated *in situ* onto these Pt substrates. The threshold for internal photoemission was found at 4.4 ± 0.2 eV, indicating that the Pt Fermi level adjusts itself precisely at midgap position of the 8.8 eV band-gap insulator. The thickness of the overlayers was controlled by a calibrated crystal monitor. During experiments, the pressure was in the lower 10^{-9} Torr range. For internal photoinjection with low energies ($\hbar\omega \leqq 6$ eV), a high-pressure Hg-Xe arc lamp and a uv monochromator were used. Injection with higher photon energies was achieved with a capillary discharge tube attached to the spectrometer. Variation of the gas used for discharge allows the excitation with photon energies of 21.2 eV (He), 16.8 eV (Ne), 11.7 eV (Ar), ~ 10.1 eV (Kr), and ~ 8.4 eV (Xe).

The analysis with the method of the topmost energy interval requires a sharp cutoff of the injected electron distribution. Capillary discharge tubes usually produce a small fraction of high-energy photons above the main excitation energy used for photoinjection. We tested the influence of this high-energy background on the determination of λ_{eff} by varying its intensity via the pressure of the gas discharge. The damping of the intensity at $E_{\max} = E_F + \hbar\omega$ appears to be independent of the intensity of the high-energy background. However, if the background is too large, with increasing overlayer thickness d, the discountinuity at $E_{\max}$ rapidly disappears in the background signal. Therefore, the spectra recorded with Kr and Xe excitation could be evaluated for $d \leqq 100$ Å only. For this reason only upper limits of λ_{eff} could be determined in these two cases.

For excitation with photon energies $\hbar\omega \geqq 8.8$ eV (ionization threshold of n-$C_{36}H_{74}$), photoionization within the overlayer occurs in addition to photoinjection. However, the top of the valence band of the alkane film is 4.4 eV below the Fermi level of the system. Therefore, injected electrons are separated from overlayer states within the topmost 4.4 eV of the electron energy distributions. Since charging effects due to the photoionization of the dielectric overlayer were not a problem at the film thicknesses used, we are not hindered to extract λ_{eff} from the topmost energy interval (Fig. 2). For $\hbar\omega \geqq 7.0$ eV, optical absorption in the overlayer has to be considered. For large d this was done by using

$$I(d)/I(0) \sim \exp[-(\mu + \lambda_{\text{eff}}^{-1})d] \tag{3}$$

instead of formula (1b). The absorption coefficient μ was extracted from optical measurements in $n-C_{36}H_{74}$ and polyethylene.[6] The correction is small, $\mu \leqq 0.2\lambda_{\text{eff}}^{-1}$.

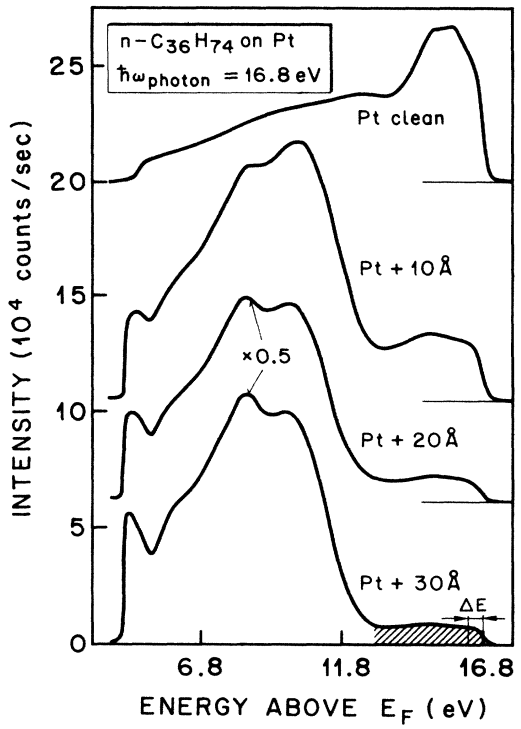

FIG. 2. Energy-distribution curves of photoelectrons emitted from Pt covered with n-$C_{36}H_{74}$ paraffine films of various thicknesses. The dark area marks the energy range of photoelectrons originating from the Pt substrate. ΔE is the energy interval used for the analysis with the topmost interval method.

III. RADIATION DAMAGE BY HOT ELECTRONS

Since the electrons used to probe the transport properties of the dielectric films can have quite significant kinetic energies, the question of electron-induced transformations in the dielectric under investigation must be addressed. Strong evidence was found that the injection of electrons with $E_{kin} \geqq 4.0$ eV ($\hbar\omega \geqq 8.5$ eV) leads to significant chemical changes of the alkane films, while no transformations were observed for $E_{kin} \leqq 3.5$ eV under our experimental conditions over days.

Firstly, the injection of electrons above a threshold energy, $E_{th} \cong 4.0$ eV, appears to stabilize the films. Unirradiated films evaporate close to the melting temperature at 76 °C under UHV conditions. Film irradiated above threshold energy, however, are stable up to about 150 °C. If hot electrons produce (C—H)-bond scission, polymerization and cross linking might occur. Both processes increase the thermal stability of the films.

Secondly, we observe that the injection of electrons above E_{th} generates a large number of new deep electron traps in the energy gap of the insulator. Trapped electrons can be exited into the conduction band either thermally or optically with subband-gap light ($\hbar\omega < E_g/2$). Since the bottom of the conduction band lies above the vacuum level, excited electrons are spontaneously emitted into vacuum and can be detected, a phenomenon usually called exoelectron emission. A detailed discussion of exoelectron emission in alkane films will be presented elsewhere. In films irradiated with light producing hot electrons below the threshold energy, only about 10^{10} electrons/cm^3 can be excited with subband-gap light. During electron injection above E_{th}, the density of detectable trapped electrons rapidly increases to about 10^{16} electrons/cm^3. This observation strongly supports the hypothesis of bond scission with subsequent polymerization and crosslink formation.

We therefore carefully investigated the influence of radiation damage on the effective mean free paths. No significant changes could be detected for irradiation doses required for the determination of λ_{eff}. We recall that λ_{eff} is extracted from the topmost energy region where the electron kinetic energies are reasonably large compared to the depth of the trap potentials. At higher doses λ_{eff} decreases by a few percent only. Therefore the measured values of λ_{eff} are considered as those of as-grown n-$C_{36}H_{74}$ films. It is clear, however, that measured values of λ_{eff} contain a small inelastic scattering contribution due to chemical damage which cannot be separated from phonon contributions. On the other hand, the small influence of chemical damage (bond scission, polymerization, cross linking) on λ_{eff} in n-$C_{36}H_{74}$ indicates that the transport of really hot electrons ($E_{kin} \gg \hbar\omega_{phonon}$) in polyethylene can be expected to be fairly similar to that observed in our model dielectric.

The electrons at the low-energy end of the spectrum, however, have thermal or nearly thermal energies and are strongly affected by the trap distribution. As can be seen from the energy distribution of transmitted electrons shown in Fig. 3, irradiation severely affects the transport of electrons with $E_{kin} \leqq 0.5$ eV. The peak on the low-

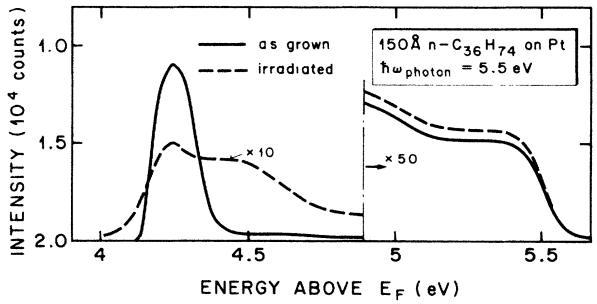

FIG. 3. Energy-distribution curves of photoelectrons emitted from Pt after traversing a 150 Å n-$C_{36}H_{74}$ paraffine film before and after irradiation with 17 eV electrons. Note the drastic decrease of transmitted intensities for low-energy electrons in the irradiated film.

energy edge of the spectrum is attributed to thermalized electrons scattered down to the bottom of the conduction band during the transport through the film. Obviously the transport of these low-energy electrons is strongly suppressed by irradiation. Low-energy electrons get trapped in irradiation-induced defects before they reach the surface of the overlayer and space charge starts to build up. If this happens, down-scattered electrons will be rejected to the substrate by the internal electric field and the low-energy electron peak does not recover even in a steady-state situation with constant density of trapped electrons. This is in fact what we observe.

Nevertheless, from what has been said before, we conclude that reliable values for the effective scattering length of n-$C_{36}H_{74}$ can be measured by the IPTA method in the electron energy range $0.5 < E_{kin} \leqq 20$ eV. Experimental results are presented in the following section.

IV. EXPERIMENTAL RESULTS

Electron energy distribution curves (EDC's) obtained with photon energies $\hbar\omega \leqq 6.5$ eV and the resulting mean free paths, λ_{eff}, are found to be in agreement with results published earlier.[4] Typical results for higher photon energies are shown in Figs. 2, 4, and 5. The variation of EDC's with overlayer thickness is shown in Fig. 2. The excitation energy is 16.8 eV (Ne I). For very thin overlayers already, the EDC's are dominated by valence-band excitations of n-$C_{36}H_{74}$. If we assume that the intensity of the alkane's valence band increases with thickness as $I(d)/I(d=\infty) = 1 - \exp(-d/\lambda_i)$ the mean information depth λ_i is found to be 20 Å. This value is in reasonable agreement with the effective mean free path derived from the damping of the intensity at the topmost energy interval shown in Fig. 4. From the slope of this curve we obtain $\lambda_{eff} \cong 20$ Å for electrons of ~ 12 eV kinetic energy. For comparison the damping of electrons with $E_{kin} \cong 1.1$ eV ($\hbar\omega = 5.5$ eV) has been measured on the same set of films. The result is included in Fig. 4: At this energy $\lambda_{eff} \cong 30$ Å. In Fig. 5 similar results with $\hbar\omega = 11.7$ eV are shown. For $d \geqq 80$ Å, the observed intensity decreases exponentially with film thickness and the slope of the high d limit, yielding λ_{eff}, is well defined [Eq. (1b)]. On

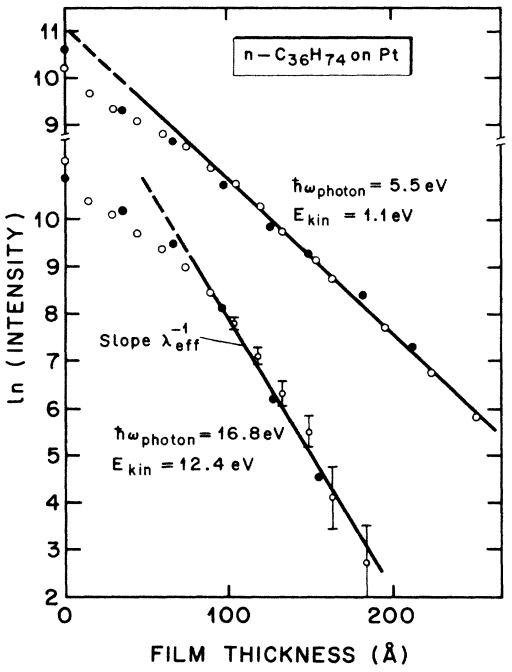

FIG. 4. Damping of photoelectrons originating from the vicinity of the Pt Fermi edge (topmost interval analysis) by the scattering in n-$C_{36}H_{74}$ overlayers. The two curves ($E_{kin}=1.1$ and 12.4 eV) are measured on the same set of films. Two independent sets of measurements are shown (○,●).

the other hand, all measurements show deviations from the exponential dependence at small d. According to Eq. (1a) an upward curvature is expected, but a downward curvature is observed. This discrepancy possibly originates from problems at the metal-dielectric interface and is not understood in detail. Since we are interested in

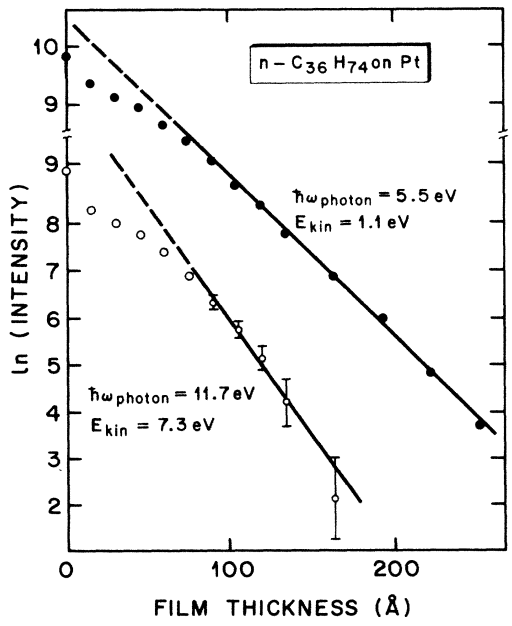

FIG. 5. Same as Fig. 4 but with $E_{kin}=7.3$ eV.

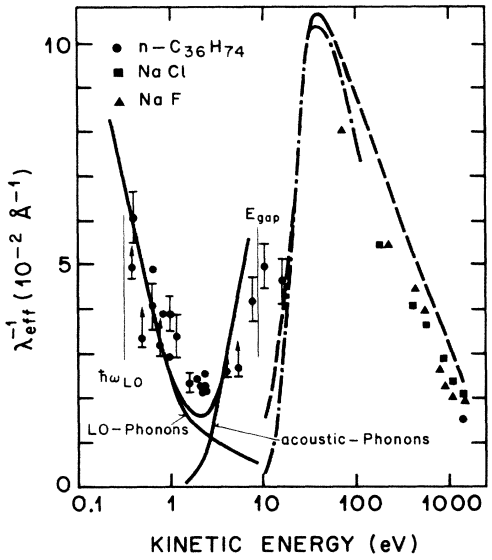

FIG. 6. Inverse effective scattering length of hot electrons in the organic insulator n-$C_{36}H_{74}$ as a function of kinetic energy (●). For comparison results in NaCl (■) and NaF (▲) from Ref. 10 are included. The pseudouniversal curve derived from measurements in inorganic insulators (dashed) from Ref. 7 and the calculated inverse effective scattering length for electron-electron scattering in polyethylene (dash-dotted) are shown. The solid lines show the inverse effective scattering length in NaCl calculated from energy and momentum relaxation frequencies published in Ref. 1. The individual contributions from optical and acoustic phonons are indicated.

λ_{eff} only, we are not hindered by this inconsistency which precludes the separation of l_u and l_p.

In Fig. 6, all experimentally determined values of the inverse effective mean free path are plotted versus electron kinetic energy. Although the real scattering rate is given by $\gamma_{eff}=\lambda_{eff}^{-1}(2E/m^*)^{1/2}$, we prefer to plot and to discuss λ_{eff}^{-1} because we do not wish to speculate on m^*. For simplicity, we will use the term "scattering rate" for λ_{eff}^{-1} in the following, and we will now discuss the energy dependence of this quantity in terms of various scattering processes in the dielectric film.

V. DISCUSSION

The scattering mechanisms for the hot electrons, such as electron-phonon and electron-electron scattering are known to be strongly energy dependent. Let us consider the contribution of electron-electron scattering to the effective scattering rate, λ_{eff}^{-1}, first.

The inelastic mean free path due to electron-electron scattering in metals has been intensively studied in the past. Similar studies in organic dielectrics are rare, especially at the kinetic energies of interest here. Experiments in metals resulted in a pseudouniversal curve with a minimum of $\lambda_{eff}\cong 10$ Å at about 50 eV kinetic energy, particularly well-known in the field of electron spectroscopy. For a review see Ref. 7.

The effective scattering rate, $\lambda_{\text{eff}}^{-1}$, may be calculated from the dielectric response function $1/\epsilon(q,\omega)$ (Ref. 8),

$$\lambda_{\text{eff}}^{-1} \sim \int \frac{1}{q} dq \, \tfrac{1}{2} \int_0^{\omega_{\max}} d\omega \, \text{Im} \left| -\frac{1}{\epsilon(q,\omega)} \right| \times \Theta(E - E_{\min} - \hbar\omega) \, . \quad (4)$$

E is the energy of the electron, q and $\hbar\omega$ are the momentum transfer and the energy involved in the transition. $E_{\min}$ is the conduction-band edge in the case of an insulator. The step function Θ and the upper integration limit

$$\omega_{\max} = \hbar/2m \, [k^2 - (k-q)^2]$$

take care of energy conservation.

The calculation of $\lambda_{\text{eff}}^{-1}$ based on the experimentally determined dielectric energy-loss function of polyethylene[9] is shown by the dash-dotted line in Fig. 6. Since the optical properties[6] and the electronic structure[5] of n-$C_{36}H_{74}$ are similar to those of polyethylene, this curve can be expected to be valid for the model compound too. The calculated curve is in reasonable agreement with the pseudouniversal curve (dashed in Fig. 6) derived from various experiments in inorganic insulators.[7] The broad maximum of the effective electron-electron scattering rates in the region between 10 and 100 eV is largely due to plasmon excitations.

For comparison, experimentally determined inverse mean free paths in NaCl and NaF (Ref. 10) as well as one point derived from the damping of the Pt $4f$ core-level intensity with n-$C_{36}H_{74}$ overlayers are included in Fig. 6. All these results indicate that the effective scattering rate of organic dielectrics can be approximated by the pseudouniversal curve derived for inorganic insulators in this high-energy range. The contribution of electron-electron scattering to $\lambda_{\text{eff}}^{-1}$ is obviously significant for electron energies $E_{\text{kin}} > 15$ eV.

We now proceed to the discussion of the high scattering rates measured below 10 eV kinetic energy. For this purpose we start with the calculation of $\lambda_{\text{eff}}^{-1}$ for the typical inorganic insulator NaCl. The effective mean free path determined in our experiment [Eq. (2)] can be written as

$$\lambda_{\text{eff}}(E) = \tfrac{1}{2} [\gamma_u^{-1}(E) \gamma_p^{-1}(E)]^{1/2} \left[\frac{2E}{m^*} \right]^{1/2} . \quad (5)$$

Using the scattering rates and the effective mass from the work of Sparks *et al.*,[1] the effective scattering rates of NaCl follow directly from Eq. (5). These authors determined energy-loss rates from the calculated energy-loss parameter, $\hbar\omega_{\text{phonon}} \gamma_u$, by setting the average phonon energy equal to the Debye energy $k_B \Theta_D$. This average phonon energy corresponds to the characteristic energy loss required for the solution of the Boltzmann equation appropriate to our experiment (see Sec. I). The effective scattering rates derived from Sparks' calculation are shown in Fig. 6 (solid line). The contributions of optical and acoustic phonons to $\lambda_{\text{eff}}^{-1}$ as well as the total scattering rates are shown. Equation (5) in this simple form is valid for isotropic scattering only, and the calculated effective scattering length is underestimated by Eq. (5) if predominant forward scattering occurs. This is possibly the case at high energies, where acoustic phonon emission dominates. However, the general trend of $\lambda_{\text{eff}}^{-1}$ is certainly correct over the whole energy range. The calculated effective scattering rates in NaCl show the same trend as our experimental results in n-$C_{36}H_{74}$.

The energy dependence of $\lambda_{\text{eff}}^{-1}$ is related to the scattering processes as follows: The large effective scattering rates measured in the vicinity of 360 meV, the approximate LO-phonon energy associated to the stretching modes of the —CH_3 and —CH_2— units,[3] arise from LO-phonon emission (Fröhlich scattering). With increasing energy $\lambda_{\text{eff}}^{-1}$ rapidly falls off due to the decrease in the LO scattering matrix element for Fröhlich scattering. Above 1.5 eV, acoustic phonon emission becomes important and dominates at high energies because of the rapid increase of the momentum scattering rate due to quasielastic deformation potential scattering. Momentum scattering thereby prevents electron runaway above the LO-phonon energies and acts as a stabilizing process on the electronic energy distribution. A similar result has been found by DiMaria *et al.* in a study of hot electrons in SiO_2.[11]

At electron energies $E_{\text{kin}} \geqq E_g = 8.8$ eV, an additional scattering channel (impact ionization) opens up. From the experimental data however, there is no clear indication that $\lambda_{\text{eff}}^{-1}$ changes significantly around 8.8 eV. Yet, the loss channel due to electron-hole pair formation is detectable in direct electron energy-loss experiments on n-$C_{36}H_{74}$.[12] If impact ionization takes place, the initial electron is scattered down in energy and disappears from the topmost energy interval. Therefore, an order of magnitude estimate of the mean ionization length of electrons with energies $E_{\text{kin}} \geqq E_g$ may be obtained by introducing an additional contribution to the inelastic phonon scattering rate arising from impact ionization $\gamma_u = \gamma_u^{\text{phonon}} + \gamma_u^{\text{ionization}}$, and by assuming that the increase of $\lambda_{\text{eff}}^{-1}$ due to impact ionization is of the order of the experimental accuracy at 8.8 eV. We further assume that the momentum scattering rate γ_p in n-$C_{36}H_{74}$ is of the same order of magnitude as in NaCl. This procedure yields a value of 100—200 Å for the mean ionization length. This value is considerably larger than the effective mean free path due to acoustic phonon emisson and some ten acoustic phonons are emitted before ionization takes place. Energy-band calculations, although imprecise for the conduction states, indicate that the phase space for impact ionization is rather restricted in saturated hydrocarbon chains.[7,13] Momentum conservation is generally not fulfilled for the transition energies, and hence λ_{eff} is controlled by acoustic phonon emission even at $E_{\text{kin}} \gtrsim E_g$.

The effective scattering rates derived from Sparks' calculation[1] are similar to those measured in n-$C_{36}H_{74}$. Hence, multiplication rates and breakdown fields in terms of avalanche breakdown are expected to be approximately the same in the two materials.[2] Experimentally determined breakdown fields for n-$C_{36}H_{74}$ (Ref. 14) as well as for NaCl (Ref. 15) are in fact both very close to 1 MV/cm. The calculated breakdown field based on our

experimentally determined scattering rates yields 1.0 MV/cm (Ref. 2) and agrees well with the directly measured values of the order of 0.9—1.4 MV/cm (Ref. 14).

Our results demonstrate that the IPTA method can be used to measure the effective scattering rate over the whole energy range relevant for dielectric breakdown. Based on the experimental results, the breakdown behavior can be predicted in terms of the avalanche breakdown model. The energy dependence of the experimentally determined effective scattering rates agree with those predicted from fundamental scattering processes such as Fröhlich scattering (LO-phonon emission) and deformation potential scattering (acoustic phonon emission) in organic dielectrics. We find that the effective scattering length for electron energies $E_{\rm kin} > 0.5$ eV is only weakly affected by radiation damage (polymerization, cross-link formation, and according electron-trap formation). In contrast, the transport of low-energy electrons, $E_{\rm kin} < 0.5$ eV, depends strongly on chemical damage. Based on these results, we may speculate on the origin of the high breakdown field in polyethylene (~ 6 MV/cm) compared to that of n-$C_{36}H_{74}$. From the radiation damage experiments it is not expected that the transport of electrons with energies $E_{\rm kin} > 0.5$ eV is significantly different in the two materials. Hence, the difference of the breakdown behavior seems to originate from the different transport properties of low-energy electrons in the two materials. Due to localization, γ_p diverges in disordered materials below the disorder localization energy which is expected to be a few tenths of an eV. This may play a substantial role for the breakdown in amorphous or partly amorphous materials such as polyethylene. Zeller[16] studied the influence of disorder localization on hot electron transport. He found that there exists a critical field at which a rapid transition from a small thermally activated hopping controlled mobility to a many orders of magnitude higher band conductivity occurs and that the avalanche would form at or near the critical field of the mobility transition.

ACKNOWLEDGMENTS

We gratefully acknowledge the fruitful collaboration and discussions we had in this field over the past few years with J. Bernasconi, H. R. Zeller, D. Mauri, J. J. Pireaux, and M. Rei Vilar. We also wish to thank W. Foditsch and R. Weder for excellent technical assistance. Finally, one of us (E. C.) is grateful to the Swiss National Science Foundation for financial support.

[1]M. Sparks, D. L. Mills, R. Warren, T. Holstein, A. A. Maradudin, L. S. Sham, E. Loh, Jr., and D. F. King, Phys. Rev. B **24**, 3519 (1981).

[2]H. R. Zeller, P. Pfluger, and J. Bernasconi, IEEE Trans. Electr. Insul. **EI-19**, 200 (1984).

[3]J. J. Pireaux, P. Thirty, R. Caudano, and P. Pfluger, J. Chem. Phys. **84**, 6452 (1986).

[4]P. Pfluger, H. R. Zeller, and J. Bernasconi, Phys. Rev. Lett. **53**, 94 (1984).

[5]J. J. Pireaux and R. Caudano, Phys. Rev. B **15**, 2242 (1977).

[6]S. Hashimoto, K. Seki, N. Sato, and H. Inokuchi, J. Chem. Phys. **76**, 163 (1982).

[7]M. P. Seah and W. A. Dench, Surf. Int. Anal. **1**, 2 (1979).

[8]H. Ibach, in *Electron Spectroscopy for Surface Analysis,* Vol. 4 of *Topics in Current Physics,* edited by H. Ibach (Springer-Verlag, Berlin, 1977).

[9]J. J. Ritsko, in *Electronic Properties of Polymers,* edited by J. Mort and G. Pfister (Wiley, New York, 1982).

[10]F. L. Battye, J. Liesegang, R. C. G. Jeckey, and J. G. Jenkin, Phys. Rev. B **13**, 2646 (1976).

[11]D. J. DiMaria, T. N. Theis, J. R. Kirtley, D. W. Dong, and S. D. Brorson, J. Appl. Phys. **57**, 1214 (1985).

[12]M. Rei Vilar, Ph.D. thesis, University of Paris VII, 1985.

[13]J. E. Falk and R. J. Fleming, J. Phys. C **6**, 2954 (1973).

[14]K. Yoshino, S. Harada, J. Kyokane, and Y. Inuishi, J. Phys. D **12**, 1535 (1979).

[15]D. B. Watson, K. C. Kao, W. Heyes, and J. H. Calderwood, IEEE Trans. Electr. Insul. **EI-1**, 30 (1985).

[16]H. R. Zeller (unpublished).